

A Review on Mechanical Properties of 3D Print Concrete Incorporating Recycled Fine Aggregate (RFA)

Adrin Ahmad Budin¹, Seyed Jamalaldin Seyed Hakim^{1*}

¹Faculty of Civil Engineering and Built Environment,
Universiti Tun Hussein Onn Malaysia, Batu Pahat, 86400, MALAYSIA

*Senior Lecturer, Faculty of Civil Engineering and Built Environment, Universiti Tun Hussein Onn Malaysia

DOI: <https://doi.org/10.30880/rtcebe.2023.04.03.033>

Received 06 January 2022; Accepted 15 May 2023; Available online 31 December 2023

Abstract 3D print concrete is an emerging construction technology and presents an opportunity for utilising materials that are otherwise considered unsuitable for concrete construction. Incorporating recycled fine aggregates from construction and demolition waste can preserve natural aggregate resources and contribute to sustainable built environment. However, the RFA as construction material in concrete mix of 3DPC is seldom applied compared to natural aggregate as construction material. Hence, this study provides a comprehensive review on the mechanical properties and structural performance of RFA, to investigate the suitability of this material to be used as construction materials. The different strategies and parameters on the behavior of 3DPC incorporating RFA such as the set-up and equipment, process, material requirement, and 3DPC parameters were determined. Moreover, the compressive strength and flexural strength are the important mechanical properties to determine the performance of 3DPC structures. Thus, the effect of 3DPC incorporating RFA on those mechanical properties and structural behavior was investigated from several journals, research paper through peer review study of the experiment and analysis was made based on its shrinkage and failure pattern characteristics. RFA have lower compressive and flexural strength, compared to natural aggregate but the difference is not significant. RFA concrete can be used in 3DPC structures design. RFA concrete has an assured quality of practicality in compressive strength and flexural strength without significant effect on strength of concrete.

Keywords: 3D concrete printing, mechanical properties, structural behaviour

1. Introduction

Construction sector accounts for 9 percent of global gross domestic product and 78.5 percent of global employment, making it among the significant contributors to economic growth [1]. Expenditures on construction rose to USD 11.4 trillion in 2018 and will reach USD 14 trillion on 2025 [2]. The fast growth of this sector necessitates a surge in the demand and supply of industrial and construction

resources like aggregate. Among most significant building material is concrete where the most common building materials consist of coarse aggregate of rock material and fine aggregate of natural sand. While natural aggregate supply is likely to provide for expansion in the coming years, excessive usage would deplete nonrenewable aggregate resources [3]. Recycled fine aggregates utilizes recycled aggregates from construction and demolition debris and industrial waste is recognized as the appropriate replacement for natural aggregate material. Moreover, construction waste solution is utilizing RFA as a building material in 3D printing. Concrete 3D printing has grown in popularity in recent years [4, 5]. When new technologies or materials emerge as alternatives, it is critical to assess their technical implications. 3D printing is a new technology that has many benefits for the environment, economics, and progression of technology application in civil structure work, according to various research studies[1, 5–8].

The aim of this study is to review the effects of 3D building materials utilizing construction and industrial waste, which is recycled fine aggregate (RFA). The study will focus on critical review on different parameter and strategies on the behavior of 3D print concrete, mechanical properties and structural behaviour of 3D print concrete incorporating RFA. The investigation on mechanical properties include the compressive strength and flexural strength incorporating RFA, which was made based on review of several journals. The structural behaviour of the 3D print concrete incorporating RFA include the analysis on shrinkage and failure pattern properties. RFA have an assured quality of shrinkage and failure pattern in compressive strength and flexural strength without significant effect on strength of concrete. Thus, can be further applied as construction material in 3DPC construction works.

2. Effect of Different Strategies and Parameters on the Behavior of 3D Print Concrete Incorporating RFA

The 3DPC strategies such as the printing set-up and technique, constrains certain material behaviours. Cementitious materials for 3DPC should be developed to match the printing approach. Achieving quantification and development of 3DPC cementitious materials required methodologies for evaluating fresh and hardened characteristics of conventional cementitious materials. Thus, several modified or innovative strategies offered in this field is summarised.

2.1 Set-up and Equipment of 3DPC

Typically, 3DPC systems in use currently include a deposition rigs, control module, and a material transfer mechanism. There are also other gantry and mechanical deposition systems with 3-/4-axis and 6-axis direction respectively [9]. The control unit controls the deposition setup to follow an operator-programmed printing route. For gantry type deposition systems, there are DOFs for motion in x, y and z plane. In contrast, the 4th DOF is attached vertically to a four-axis gantry robot to provide rotation. Industrial robotic arms, unlike three- and four-axis gantry type deposition systems, have four to six rotating degrees of freedom [10]. A mixing machine, pump, and printer are the components of a material conveyance system that prepares, pumps, and extrudes new mixes. So the necessity for a 3D printer that can create commercial ready-mixed concrete has risen dramatically. Proposal by researcher on a column-type mechanical construction with a four-column frame for 3D printing [11]. Structure of 3D printer as shown in Figure 1, the column-type concrete 3D printer is easy to set up and can produce constructions up to six storeys. The concrete pump truck's print head and arm are also separately operated and each has a positioning sensor that detects their relative location. When the print head is continually printing concrete, the concrete pump truck's arm may independently position and feed the concrete. Three-dimensional printers can use the column-type mechanical construction, but the key challenge is developing a printer that can print ready-mixed concrete.

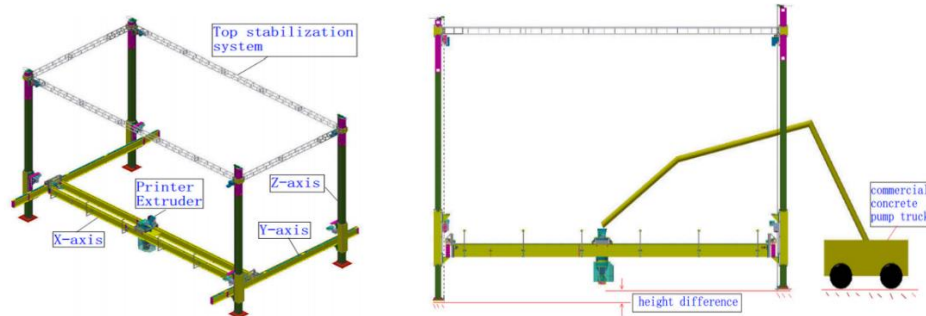


Figure 1: Column-type 3D printer for ready-mixed concrete axonometric & elevation view [11].

2.2 Process of 3DPC

In this study, the process design of 3DPC involves integrated process of printing from raw material input to finished product output [12]. Figure 2, show the design process from model design, slicing and tool path then to the mix design and finally input the printing parameter design for further processing of output.

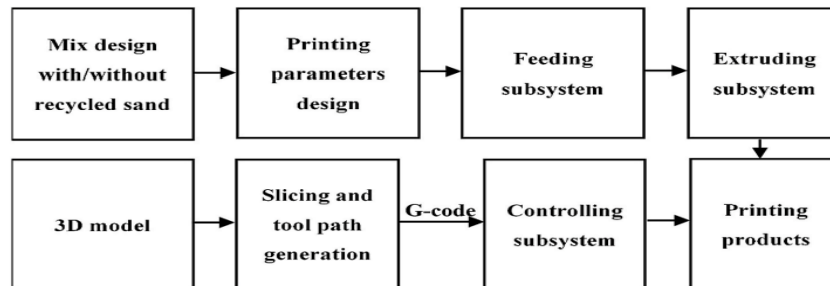


Figure 2: Design process of 3DPC [12].

2.3 Material Requirement for 3DPC

The existing 3D printing construction technologies may be split into three groups based on building material diversity: Stratified squirting using cement-based substance, then, using aggregate powder as a building material. A big manipulator, layered bonding and three-dimensional building approach [13]. Special restrictions for construction materials are imposed by 3D printing technologies. Printing also affects structural and material hardening properties. The impact of 3D printing is thus reliant on the rheological, plasticity, and self-condensation qualities of cement-based materials, as well as the equipment and building process compatibility. Given that aggregate makes up over 70 percent of the overall volume of cement-based materials, its performance impacts extrusion, printing, mechanical properties and 3D printing durability.

Wolfs [10], described two basic material preparation strategies. For the material conveying pump hopper, the new mix is first prepared in batch afterward by manual or mechanically supplied. This method is suited for small-scale applications, such as the production of printed materials and other research projects. On the other hand, large-scale building requires a continuous system. Diverse mixing procedures may need diverse fresh mixes. Fresh mixing with longer open time or printability windows may be required for the former. Also, in order to produce homogeneous components, low filaments must be link with higher filaments. For this reason, the ready-mixed concrete must be able to print a specified layered structure or thickness. Workability and mix proportions affect buildability [11].

The proportions of binders and aggregates in 3D printing cement-based materials are similar in traditional materials. As the wet mix of 3D printing materials is mixed, pumped, and deposited layer at

a time, high-performance materials are needed. As with standard materials, the ratio of binder to aggregates might vary. Research of diverse cementitious materials, of mortar including standard mixture of mortar, geo-polymer, fiber-mixed, and nanoparticle-mixed, have been effectively utilize with 3DPC [14]. However, most studies employ sand as fine aggregate, and just a few use coarse aggregate [15]. Table 1, outlines the researchers 3D printed material mix compositions. As can be seen, binders are utilised in much larger volume.

Table 1: Mix composition of 3DPC components utilizes from various studies [15].

Authors	Binders (kg/m ³)	Aggregates (kg/m ³)	Water (kg/m ³)	Others (kg/m ³)
Kruger et al., 2020	827	1167 (max size 4.75 mm)	261	SP: 12.2
Panda and Tan, 2018	856	869 (max size 2 mm)	66	Alkaline reagent: 356
Nerella and Mechtcherine, 2019	780	1240 (max size 2 mm)	180	SP: 10
Paul et al., 2018	713	1212 (max size 2 mm)	285	Sodium lignosulfonate 7
Khalil et al., 2017	683	850 (max size 2 mm)	236	SP: 1.76
Chen et al., 2019	826	1242 (max size 2 mm)	248	PCE: 17, VMA: 2
Ogura et al., 2018	W/B = 0.22-0.24; S/B = 0.2-1.2; Fiber (% , Vol) 0.3-1.5			
Marchment et al., 2019	W/B = 0.36; S/B = 1.5			

2.4 3DPC Parameters

According to Chen et al. [16] different printing settings may alter the 3DPC material interlayer bonding. The respective parameters were chosen and addressed in this research.

2.4.1 Nozzle Type

Factors in nozzle of 3DPC involve the flow direction (down-flow, back-flow, or a combination of both), opening size, and shape (e.g., round or rectangle). This is especially true as the nozzle standoff distance is lower than the nozzle opening's breadth or diameter. The nozzle may impart additional force to the deposited layer. The pressed layer procedure may improve compaction and contact regions between layers. The squeezing force should decrease as the deformation of layer increases the standoff distance of nozzle. Nonetheless, the ideal 3DPC nozzle remains a concern for further research as the set of experiments is required to quantify how these factors affect binding strength and printability.

2.4.2 Nozzle Standoff Distance

Layer deformity is inevitable, therefore maintaining the standard nozzle standoff distance during printing is difficult. Increasing substrate deformation increases nozzle standoff distance. Lengthening the standoff distance of nozzle raises inaccuracy in deposition of layer, affecting the pressure and area

of contact. Thus, interlayer connections may be affected [9]. Studies on the impact of nozzle standoff lengths on interlayer bonding [17]. Bond strength is reduced by over 30 percent by increasing nozzle standoff distance [18]. This parameter has a less substantial influence on the overall strength of interlayer bonding, according to [9, 17]. In their research, raising the nozzle height from the default setting only increased the standard deviations. The varying impacts across experiments may be attributable to material and printing setting variations, notably nozzle types.

2.4.3 Time Interval

The duration of time between two successive layers is a significant printing element affecting buildability and interlayer bond strength, which known as time interval. Lengthening the time between layers improves layer shape stability but reduces interlayer bond strength [9, 17]. Tay et al. [19] found a significant relationship between material storage modulus variation and interlayer bonding strength within short time periods (1–20 min). They found that for given printing parameters like speed and nozzle standoff distance, duration for printed cementitious materials to set and prevent cold-joint is influenced by their structuration rate and plastic viscosity. Enlarging the time gap between layers may cause air voids to grow in the interface area causes the bonding strength of interlayer reduces [16].

2.4.4 Curing Condition

In practical, large-scale construction elements may need many printing processes. The extended time delay across sessions might be from several hours to one day. It is possible that the printing environment affects interlayer bonding [9]. Interlayer bonding in printed samples may be affected by curing conditions of humidity and ambient temperature in first layer. Temperature and humidity might affect how quickly deposited materials dry. Exposing the substrate to a drying environment may significantly reduce binding strength [20].

2.4.5 Interlayer

In addition to using appropriate printing conditions, there are two major strategies used to improve the bonding strength of interlayer on the 3DPC layers surface connection. Firstly, by expanding the layer surface of contact, the absence of functional contact regions between layers causes excessive void content at the connection. Interlocking between two following layers increased effective contact areas and interlayer bond strength [21]. Likewise, use a combing to roughen the placed layer's surface and manually join the layers. Additionally, application of cellulose fibre acting as internal curing agent and fine limestone filler is used to improve the layer's workability and hydration.

3. Effect of 3D Print Concrete Incorporating RFA as Partial Replacement of Natural Aggregate on Compressive and Flexural Strength of 3DPC

All of the following factors of the different strategies and parameters on the behavior of 3D print concrete incorporating RFA mentioned previously should be considered while presenting an overview on 3DPC cementitious materials. Therefore, understanding the materials behaviour involves an analysis of mechanical properties and the structural behaviour that influence them. Nonetheless, the study of rheological properties perhaps a challenging one because of the many elements that influence concrete fresh characteristics. In this study, compressive strength and flexural strength of 3DPC incorporating RFA was review.

3.1 Compressive Strength

In the research by Xiao et al. [22] the compressive strength of 3DPC and mold-casted specimens incorporating RFA were study. In the research findings, 3DPC samples had a compressive strength of 84.9 percent of mould cast samples of the similar combination at room temperature. RFA had a detrimental influence on the mechanical properties of 3DPC samples, compared to 3DP-N and 3DP-NR, the compressive strength of 3DP-NR fell by 22.6 percent. While, the compressive strength of MC-

N and 3DP-N exhibited a comparable decline pattern as temperature increased. The inclusion of RFA offers advantages to limit the exponential spalling and the heat resistance of compressive strength.

In another research, on the 3DPC incorporating waste material by Bai et al. [23] the failure on the buildability of the 3DPC incorporating RFA shown three modes of failure from the compressive test on the specimen which are the buckling, collapsing and shear failures. The improvement of the material early stiffness with precise printing settings, followed by a steady layer stacking procedure, helps prevent collapse failures. This study attempts to evaluate and estimates the buildability of the 3DPC incorporating RFA during the early printing stage, before the first setup under compression test as shown in Figure 3.

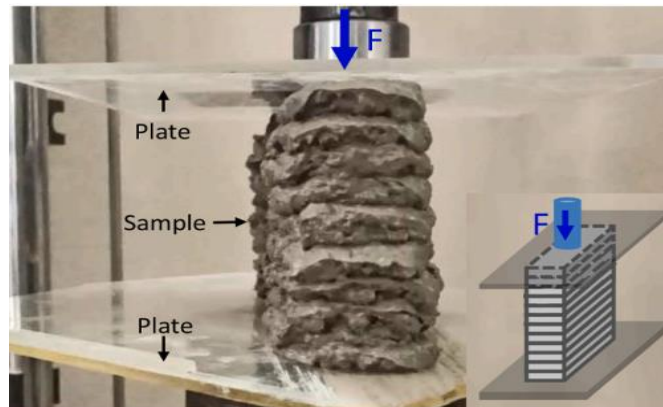


Figure 3: Compression test for 3DPC incorporating RFA [23].

Comparative, on the NCA mortar was tried. The test findings show that the aggregate gradation composition have a substantial impact towards printed material compressive strength. In the first stage of the constructive bearing capacity, the materials possess high bearing capacity and low deformation, under compression, the region fulfills buildability of 3DPC. After the ultimate bearing capacity is attained, the mid-term bearing capacity is reached. As a result of this, the load-bearing capacity changes little, but in material failure region, the created structure is progressively damaged. The materials interior particle sizes condense and increases their load-bearing capability in loading stage. The printed material's constructive load-bearing characteristic curve is S-shaped. Therefore, as compressive loading increased, so did layer loading during printing.

3.2 Flexural Strength

Xiao et al. [22] research on incorporating RFA in 3DPC in different temperature primarily in elevated temperature. The research result show at room temperature, 3DPC samples had lesser flexural strength at 20 percent than MC-N samples. In addition, the 3DP samples flexural stiffness, fracture energy, flexural strength before the first crack and maximum flexural strength are govern by the RFA presence with a significant impact as previous researched [4]. Furthermore, with addition of RFA, it lessen the flexural strength before the first breakdown of the 3DP specimen. Once that PE fibre concentration was low, like 0.25 percent, adding RFA lessen the 3DP specimen flexural strength. The specimen flexural strength lower by 33–50 percent as the specimen applied load along X, Y, and Z directions.

The finding was expected given earlier research on the influence of RFA on with specimens undergoes bending [24]. Just as the PE fibre concentration was high, like 1.4 percent, the inclusion of RFA had no influence on the 3DP specimen flexural strength, and a portion of samples has stronger flexural strength compare to samples without RFA. Considering flexural strength was predominantly regulated with fibre pull-out, the porous RFA had a limited influence on flexural strength [5, 25]. The RFA lessen the specimen flexural rigidity. The results confirmed that 3DPC incorporating RFA had a lesser elastic modulus than normal concrete [26]. The stiffness of the 3DP specimen is linked to the

aggregate and mortar stiffnesses, porosities, and interfacial bonds [27]. A cement paste was added to the RFA mixture in this research. As indicated in Table 2, RFA absorbed more water and had a lower apparent density than natural aggregate owing to its high porosity.

Table 2: Basic properties of the RFA and natural fine aggregate [4].

Sand	Fineness modulus	Maximum particle size (mm)	Apparent density (kg/m^3)	Loose/dense packing density (kg/m^3)	Moisture content (%)	Water absorption (%)
Natural aggregate	1.62	0.9	2586.5	1399/1491	0.2	1.0
RFA	1.53	0.9	2410.7	1014/1070	0.6	15.0

The form and microstructure of RFA compare to the natural sand are thought to have influenced the mechanical findings. The SEM result of a 3D printed specimen made of RFA. As a consequence, the samples microstructure was loosened and its compactness decreased with RFA [4]. Interfacial micro-cracks between RFA and these cement pastes might cause early flaws in 3D printed specimens. Dimension and stickiness of interfacial transition region connecting cementitious material and aggregate also affect mechanical characteristics of printing materials. The mechanical characteristic of concrete were affected by void structure. These results show that adding RFA to 3D printed concrete enhances porosity. In the RFA, the result in gap between fine aggregate is due to associated cementitious material and surface roughness. Thus, improving the void structure may increase the performance of 3DPC.

4. Effect of Incorporating RFA on Shrinkage and Failure Pattern of 3DPC

While, it is only a few for research on the shrinkage and failure pattern properties of 3DPC. Several researches have studied the material properties and structural behavior of 3DPC. It can be concluded that the studies of the mechanical properties and structural behavior of 3DPC is a critical goal to understand the practicability of 3DPC incorporating RFA technique in engineering application.

4.1 Shrinkage

The absence of aggregate and high cementitious content in 3DP materials causes the micro shrinkage fractures are commonly produced [23]. Adding coarse aggregate help reduces shrinkage of 3DP. The material shrinkage as the ambient temperature and relative humidity vary during the initial and curing phases. Concrete shrinkage complicates 3D printing because standard concrete setting time and fluidity are limited, without liquid stage filling up shrinkage spaces. Furthermore, early shrinkage is focused around 0–8 h after water mixing, suggesting a severe potential danger for 3D concrete materials. According to Tran et al. [28] 3DPC constructions are subjected to rapid shrinkage due to self-drying, plastic shrinkage and drying. Consequently, along the rheology box printability, the ideal concrete compositions for printing should have minimal shrinkage. This is a concern when constructing a 3D printed concrete mix.

In this study, 7 effective concrete printing compositions were tested and analysed for shrinkage. Modified ASTM C1581 were used to perform the shrinkage testing, where the shrinkage strain was evaluated 3 hours after casting. Table 3 presents the maximum stresses and ages at cracking for 7 successful concrete mixes for printing also it shows that adding PP fibre, increasing S/B, and increasing W/B improves the concrete's resistance to shrinkage cracking.

Table 3: Shrinkage results of seven successful concrete mixtures for 3DPC [28].

Mix	W/B	PP fiber (kg/m ³)	μ (Pa.s)	τ_o (Pa)	Age at cracking (Days)	Maximum strain ($\mu\epsilon$)	Strain at (%)		Coefficient of variation (%)
							12h	24h	
M3	0.26	0	23.3	510.1	1.75	46.35	66	83	5.1
M8	0.26	1.35	45.3	668.6	1.85	62.12	62	81	4.6
M14	0.28	2.7	12.9	180.7	1.96	71.45	71	88	4.9
M19	0.28	5.4	22.3	256.6	1.98	74.95	69	85	5.4
M21	0.22	0	69.9	376.4	1.83	49.85	87	96	5.8
M32	0.24	2.7	48.2	251.4	3.58	78.56	32	58	4.2
M37	0.24	5.4	58.9	498.2	4.62	87.23	29	52	3.8

Additionally, the 3D printed concrete shrinks 96 percent in the first 24 hours after casting, compared to the peak shrinkage during concrete fracture. Using 1.35 kg/m³ PP fibre increased age at concrete cracking from 1.75-1.85 days and maximum strain at cracking from 46.35-62.12. The maximum cracking strain is the steel ring compressive strain caused by concrete shrinkage. Its compressive strain is equal to the tensile strain of its concrete counterpart. Thus, the highest tensile strain causes concrete fracture during shrinkage. The result from Table 3 further reveals that concrete with a W/B ratio of 0.22 shrinks quicker and has worse shrinkage cracking resistance. Especially, the concrete shrinkage in the first 24 hours consumes 96 percent of total shrinkage, this issue starts a problem that the printed structures might have fractures if no proper curing procedure used to the printed concrete items at an early age. All three types of fibres have a substantial impact on the rheological properties and shrinkage cracking resistance of concrete. A good rheological qualities and shrinkage cracking resistance should be balanced to achieve an optimal concrete mixture for 3DP. The studies confirmed that adding PP fibre, increasing S/B, and increasing W/B improves the concrete's resistance to cracking. The shrinkage of 3DPC is up to 96 percent in the first 24 hours after casting, compared to the maximum shrinkage at concrete cracking.

Shahmirzadi et al. [29] has conducted similar research on the effect of relative humidity and temperature on shrinkage and related mechanical and physical characteristics of 3D printed mortars. Where, in this study, the S/C 0.8 and 1.0 free-formed and conventionally cast mixes were used. The specimens with S/V ratios of 1.67 cm⁻¹ and 1.125 cm⁻¹ were measured for shrinkage strain. This study concluded that for a given S/V ratio and curing period, raising the S/C ratio of a printed mortar from 0.8 to 1.0 reduced the drying shrinkage strain of control and free-formed specimens (10 percent). The shrinkage deformation of free formed specimens reduced nearly 2.5 times when cured in tropical conditions (35°C and 85 percent RH). This study also found that in printing combinations with high cement concentration, autogenous shrinkage may account for up to 30 percent of overall shrinkage. Further study is required to determine the impact of high temperature curing on autogenous shrinkage. Regardless of S/C ratio, overall porosity of free-formed specimens was lower at 112 days, compared to conventional cast samples. During the same time frame, the free-formed specimens developed finer pores. These findings matched the shrinkage strain of free-formed specimens and demonstrated that increased shrinkage strain at later ages was due to excessive water loss and reduced total pore volume. Additionally, excess moisture loss may produce micro-cracking in cement paste, resulting in reduced compressive strength of free-formed specimens compared to control specimens. The results show that environmental factors, mix design optimization (e.g. optimising S/C ratio), and printing filament size affect the shrinkage development of 3DP cementitious materials. A baseline for future research on shrinkage strain development and structural integrity of printed items under varied curing condition and shrinkage compensating admixtures in 3DP mixes. Determining the influence of non-uniform shrinkage on the structural integrity of printed items requires greater study into the shrinkage development of 3DP

components in response to variations in internal relative humidity inside or between printing filaments. A detailed study of the effects of chemical shrinkage, hydration rate, and high temperature curing on autogenous shrinkage of 3DP mixtures is also suggested.

4.2 Failure Pattern

Based on the research result, RFA had no impact on the crack spreading and failure pattern of 3DPN and 3NPR specimens since both specimens failed suddenly as the load reached their maximum bearing capacity [30]. Along the loading direction, the primary crack also along progression. Comparing 3DPR and 3DPRF specimens revealed the influence of fibres on crack progression and failure pattern. Generally, specimen 3DPR exhibited very little deformation at the bottom before collapse, with no visible fissures. This shows 3DPN and 3NPR brittle failure in flexural test. However, 3DPRF with 100 percent RFA and 1 percent fibres demonstrated severe deformation and broad fractures after failure. Moreover, initial and other fractures may be seen appearing, developing, and propagating under loading. Deformation of 3DPRF under bending is shown by the separated displacement field with maximum displacement of 3.7038 mm. The displacement indicating that fiber-reinforced specimen fractures cannot spread to the top even if they are quite broad at the bottom.

Adding fibres converts the 3DP specimen from brittle to ductile failure in the flexural test. Ding et al. [25] found that during testing, the early age specimens showed two primary characteristic failure patterns under uniaxial compressive stresses. During this time span, RFA has relatively little influence on the specimen failure pattern. Because of the shear fracture structure, the specimen was able to withstand significant pressures. However, the specimen's stiffness operated on the lateral direction of the compressive force, preventing tensile tension. The shear plane formed when the particle cohesiveness was exceeded. This behaviour is also seen in cohesive soil tests [31]. The emergence of shear fractures in cement-based 3D printed materials indicates the commencement of the setting process from green strength to compressive strength [25]. The failure pattern appeared mostly on early age specimens, showing that the material was plastic and malleable at this point. The shearing plane angle rose with time and percentage of RFA replacement. The shear fracture occurred sooner when additional RFA was applied. Results implies that the use of RFA accelerates the early age progression of strength in maturity of specimens.

5. Conclusion

In this study, the available technical paper involving the 3DPC incorporating RFA materials from construction and demolition waste, and industrial waste were reviewed. The different strategies and parameters on the behavior of 3DPC incorporating RFA were researched, critical review on the effect of incorporating RFA as partial replacement of natural aggregate on compressive and flexural strength of 3DPC were investigated including the critical review on shrinkage and failure pattern properties.

The technical studies showed the strategies that typical in 3DPC is extrude of materials with higher or adequate stiffness. Whereby, a controlled extrusion of high pumping pressure can be controlled with the stress yield and plastic viscosity of extrusion material. The interlayer bonding strength of 3DPC may be affected parameters such as curing condition, sets intervals, nozzle types and distance of nozzle standoff. The recent approaches with enlarging the connection surface area is helpful in improving the interlayer bonding strength of 3DPC, and the adhesion between layers.

From this study, the compressive strength of the 3DPC incorporating RFA, show advantages in limiting the exponential spalling and the heat resistance of compressive strength. While for the flexural strength, incorporation of RFA in 3DPC lessen the flexural stiffness and strength of 3DP samples. Moreover, the microscopic resulted the formation and microstructure of RFA that affected the mechanical properties of 3D printed samples. The surface of the RFA was found out to be affix to loose old cement paste, causing the formation of porous structure and high water absorption capabilities. RFA

may be utilised to build 3DPC structures rather than natural aggregate in practical situations when deformation and stiffness requirements are not as stringent.

From the analysis on the shrinkage and failure pattern properties of 3DPC incorporating RFA, it exhibits with vary gradations and size range, the 3DP process and aggregate type unfavorably affected the shrinkage properties of the 3DPC. It is affected also by various factors such as aggregate light-weight, relative-humidity and curing time. Moreover, the existence of RFA in between the layers help increasing the area of contact on surface which increase the interlayer bond subsequently. Next, the incorporation of RFA in 3DPC show a slight effect on the failure pattern while, with an addition of fibre reinforcement will help change the 3DPC failure pattern from brittle to ductile regardless in compression or tension. An addition of additives may reduce the negative impact of RFA.

Acknowledgement

The authors would like to thank the Faculty of Civil Engineering and Built Environment, University Tun Hussein Onn Malaysia for its support.

References

- [1] M. A. Hossain, A. Zhumabekova, S. C. Paul, and J. R. Kim, "A review of 3D printing in construction and its impact on the labor market," *Sustain.*, vol. 12, no. 20, pp. 1–21, 2020, doi: 10.3390/su12208492.
- [2] D. best Raynor, "Construction spending globally 2014-2035," 2020. [Online]. Available: <https://www.statista.com/statistics/788128/construction-spending-worldwide/#statisticContainer>.
- [3] S. Ismail, K. W. Hoe, and M. Ramli, "Sustainable Aggregates: The Potential and Challenge for Natural Resources Conservation," *Procedia - Soc. Behav. Sci.*, vol. 101, pp. 100–109, 2013, doi: 10.1016/j.sbspro.2013.07.183.
- [4] T. Ding, J. Xiao, S. Zou, and J. Yu, "Flexural properties of 3D printed fibre-reinforced concrete with recycled sand," *Constr. Build. Mater.*, vol. 288, p. 123077, 2021, doi: 10.1016/j.conbuildmat.2021.123077.
- [5] T. Ding, J. Xiao, S. Zou, and Y. Wang, "Hardened properties of layered 3D printed concrete with recycled sand," *Cem. Concr. Compos.*, vol. 113, p. 103724, Oct. 2020, doi: 10.1016/j.cemconcomp.2020.103724.
- [6] J. Biernacki *et al.*, "Cements in the 21 st Century: Challenges, Perspectives, and Opportunities," *J. Am. Ceram. Soc.*, vol. 100, 2017, doi: 10.1111/jace.14948.
- [7] M. Sakin and Y. C. Kiroglu, "3D Printing of Buildings: Construction of the Sustainable Houses of the Future by BIM," in *Energy Procedia*, Oct. 2017, vol. 134, pp. 702–711, doi: 10.1016/j.egypro.2017.09.562.
- [8] S. Paul, G. van Zijl, M. J. Tan, and I. Gibson, "A review of 3D concrete printing systems and materials properties: current status and future research prospects," *Rapid Prototyp. J.*, vol. 24, p. 0, 2018, doi: 10.1108/RPJ-09-2016-0154.
- [9] Y. Chen, K. Jansen, H. Zhang, C. Romero Rodriguez, Y. Gan, O. Çopuroğlu, E. Schlangen, "Effect of printing parameters on interlayer bond strength of 3D printed limestone-calcined clay-based cementitious materials: an experimental and numerical study," *Constr. Build. Mater.*, 2020.
- [10] R. Wolfs, "Experimental characterization and numerical modelling of 3D printed concrete," *Eindhoven Univ. Technol.*, 2019.
- [11] G. Ji, T. Ding, J. Xiao, S. Du, J. Li, and Z. Duan, "A 3D printed ready-mixed concrete power

- distribution substation: Materials and construction technology,” *Materials (Basel)*, vol. 12, no. 9, 2019, doi: 10.3390/ma12091540.
- [12] J. Xiao *et al.*, “3D recycled mortar printing: System development, process design, material properties and on-site printing,” *J. Build. Eng.*, vol. 32, no. September, p. 101779, 2020, doi: 10.1016/j.jobe.2020.101779.
- [13] Z. Zhao, S. Remond, D. Damidot, and W. Xu, “Influence of fine recycled concrete aggregates on the properties of mortars,” *Constr. Build. Mater.*, vol. 81, pp. 179–186, Apr. 2015, doi: 10.1016/j.conbuildmat.2015.02.037.
- [14] A. Williams, “Berkeley Researchers Pioneer New Powder-Based Concrete 3D Printing Technique,” *New Atlas*, 2015.
- [15] J. Zhang, J. Wang, S. Dong, X. Yu, and B. Han, “A review of the current progress and application of 3D printed concrete,” *Compos. Part A Appl. Sci. Manuf.*, vol. 125, no. April, p. 105533, 2019, doi: 10.1016/j.compositesa.2019.105533.
- [16] Y. Chen, S. He, Y. Gan, O. Çopuroğlu, F. Veer, and E. Schlangen, “A review of printing strategies, sustainable cementitious materials and characterization methods in the context of extrusion-based 3D concrete printing,” *J. Build. Eng.*, vol. 45, no. February 2021, p. 103599, 2022, doi: 10.1016/j.jobe.2021.103599.
- [17] R. J. M. Wolfs, F. P. Bos, and T. A. M. Salet, “Hardened properties of 3D printed concrete: The influence of process parameters on interlayer adhesion,” *Cem. Concr. Res.*, vol. 119, pp. 132–140, May 2019, doi: 10.1016/j.cemconres.2019.02.017.
- [18] B. Panda, S. C. Paul, N. A. N. Mohamed, Y. W. D. Tay, and M. J. Tan, “Measurement of tensile bond strength of 3D printed geopolymers mortar,” *Meas. J. Int. Meas. Confed.*, vol. 113, pp. 108–116, Jan. 2018, doi: 10.1016/j.measurement.2017.08.051.
- [19] M. J. T. Y.W.D. Tay, G.H.A. Ting, Y. Qian, B. Panda, L. He, “Time gap effect on bond strength of 3D-printed concrete,” *Virtual Phys. Prototyp.*, vol. 14, pp. 104–113, 2019, [Online]. Available: <https://doi.org/10.1080/17452759.2018.1500420>.
- [20] N. Roussel, “Rheological requirements for printable concretes,” *Cement and Concrete Research*, vol. 112. Elsevier Ltd, pp. 76–85, Oct. 01, 2018, doi: 10.1016/j.cemconres.2018.04.005.
- [21] B. K. B. Zareiyan, “Effects of interlocking on interlayer adhesion and strength of structures in 3D printing of concrete,” *Autom. Constr.*, 2017, [Online]. Available: <https://doi.org/10.1016/j.autcon.2017.08.019>.
- [22] J. Xiao, N. Han, L. Zhang, and S. Zou, “Mechanical and microstructural evolution of 3D printed concrete with polyethylene fiber and recycled sand at elevated temperatures,” *Constr. Build. Mater.*, vol. 293, p. 123524, 2021, doi: 10.1016/j.conbuildmat.2021.123524.
- [23] G. Bai, L. Wang, G. Ma, J. Sanjayan, and M. Bai, “3D printing eco-friendly concrete containing under-utilised and waste solids as aggregates,” *Cem. Concr. Compos.*, vol. 120, no. October 2020, p. 104037, 2021, doi: 10.1016/j.cemconcomp.2021.104037.
- [24] C. S. P. S.C. Kou, “Properties of self-compacting concrete prepared with coarse and fine recycled concrete aggregates,” *Chem. Concr. Res.*, vol. 31, pp. 622–627, 2009.
- [25] T. Ding, J. Xiao, F. Qin, and Z. Duan, “Mechanical behavior of 3D printed mortar with recycled sand at early ages,” *Constr. Build. Mater.*, vol. 248, p. 118654, 2020, doi: 10.1016/j.conbuildmat.2020.118654.
- [26] E. Dapena, P. Alaejos, A. Lobet, and D. Perez, “Effect of Recycled Sand Content on Characteristics of Mortars and Concretes,” *J. Mater. Civ. Eng.*, vol. 23, pp. 414–422, 2011, doi:

10.1061/(ASCE)MT.1943-5533.0000183.

- [27] L. Evangelista and J. de Brito, “Mechanical behaviour of concrete made with fine recycled concrete aggregates,” *Cem. Concr. Compos.*, vol. 29, no. 5, pp. 397–401, May 2007, doi: 10.1016/j.cemconcomp.2006.12.004.
- [28] Tran, Mien V., Yen T.H. Cu and C. V. H. Le, “Rheology and shrinkage of concrete using polypropylene fiber for 3D concrete printing,” *Build. Eng.*, 2021.
- [29] A. K. Shahmirzadi, Mohsen Rezaei, Aliakbar Gholampour and T. D. Ngo, “Shrinkage behavior of cementitious 3D printing materials: Effect of temperature and relative humidity,” *Cem. Concr. Compos.*, 2021.
- [30] J. Xiao, S. Zou, T. Ding, Z. Duan, and Q. Liu, “Fiber-reinforced mortar with 100% recycled fine aggregates: A cleaner perspective on 3D printing,” *J. Clean. Prod.*, vol. 319, no. February, p. 128720, 2021, doi: 10.1016/j.jclepro.2021.128720.
- [31] S. P. S. T. Voigt, T. Malonn, “Green and early age compressive strength of extruded cement mortar monitored with compression tests and ultrasonic techniques,” *Chem. Concr. Res.*, vol. 36, pp. 858–867, 2006.